

The effects of stellar population synthesis on the distributions of the asteroseismic observables ν_{max} and $\Delta\nu$ of red-clump stars

Wuming Yang^{1,2*}, Xiangcun Meng¹ and Zhongmu Li^{3,4}

¹*School of Physics and Chemistry, Henan Polytechnic University, Jiaozuo 454000, Henan, China.*

²*Department of Astronomy, Beijing Normal University, Beijing 100875, China.*

³*Institute for Astronomy and History of Science and Technology, Dali University, Dali 671003, China.*

⁴*National Astronomical Observatories, Chinese Academy of Sciences, Beijing 100012, China.*

ABSTRACT

The distributions of frequencies of the maximum oscillation power (ν_{max}) and the large frequency separation ($\Delta\nu$) of red giant stars observed by CoRoT have a dominant peak. Miglio et al identify that the stars are red-clump stars. Using stellar population synthesis method, we studied the effects of Reimers mass loss, binary interactions, star formation rate and the mixing-length parameter on the distributions of ν_{max} and $\Delta\nu$ of red-clump stars. The Reimers mass loss can result in an increase in the ν_{max} and $\Delta\nu$ of old population which lost a considerable amount of mass, but lead to a small decrease in those of middle-age population which lost a little bit of mass. A high mass-loss rate impedes the low-mass and low-metal stars evolving into core-helium burning stage. Both Reimers mass loss and star formation rate mainly affect the number of CHeB stars with ν_{max} and $\Delta\nu$, but have almost no effect on the peak locations of the ν_{max} and $\Delta\nu$. Binary interactions also can lead to that the ν_{max} and $\Delta\nu$ of some stars increase or decrease. But the fraction of CHeB stars undergoing binary interactions is very small in our simulations. Thus the peak locations are also not affected by binary interactions. The nonuniform distributions of the ν_{max} and $\Delta\nu$ are mainly caused by the most of red-clump stars having an approximate radius rather than mass. However, the radius of red-clump stars decreases with increasing the mixing-length parameter. Thus the peak locations of the ν_{max} and $\Delta\nu$ can be affected by the mixing-length parameter.

Key words: stars: mass-loss; stars: fundamental parameters; galaxy: stellar content; stars: oscillations

1 INTRODUCTION

Solar-like oscillations have been confirmed in many main-sequence and subgiant stars, such as α Cen A (Bedding et al. 2004), α Cen B (Kjeldsen, Bedding & Butler 2005), Procyon A (Eggenberger et al. 2004), η Bootis (Carrier, Eggenberger & Bouchy 2005), etc. Some giant stars, such as ξ Hya (Frandsen et al. 2002), η Ser (Barban et al. 2004), and ϵ Oph (De Ridder, Barban & Carrier 2006), have also been shown to oscillate. Asteroseismology is a powerful tool for determining the fundamental parameters of individual stars (Eggenberger, Carrier & Bouchy 2005; Eggenberger & Carrier 2006; Yang & Meng 2010), and it has significantly advanced the theory of stellar structure and evolution.

The detection of solar-like oscillations in red giant stars opened up a new field that can be explored with asteroseismic techniques. For an ensemble of cluster stars all having the same age and metallicity, studying oscillations in the cluster stars should provide more constraints on stellar structure and evolution theory than just fitting parameters of single oscillating stars (Stello et al.

2007). Thus a number of attempts have been made to detect solar-like oscillations in giant stars of clusters (Gilliland et al. 1993; Gilliland 2008; Edmonds & Gilliland 1996; Stello et al. 2007; Frandsen, Bruntt Grundahl 2007; Stello & Gilliland 2009; Stello et al. 2010; Bedding et al. 2010). The oscillations of giant stars have been detected in a few clusters, such as open cluster M67 (Stello et al. 2007), globular cluster 47 Tucanae (Edmonds & Gilliland 1996) and NGC 6397 (Stello & Gilliland 2009). However, these observations did not obtain oscillation frequencies. Recently, using the data observed by the first CoRoT (Baglin et al. 2006) 150-day long run in the direction of the galactic centre (LRc01), Hekker et al. (2009) obtained the frequencies of maximum oscillation power (ν_{max}) and the large separations ($\Delta\nu$) of about 800 solar-like oscillating red giants. They found that distributions of the ν_{max} and $\Delta\nu$ are non-uniform (see Fig. 1), which provide an opportunity for detailed studies of population of galactic-disk red giants (Miglio et al. 2009). Additionally, theoretical ν_{max} and $\Delta\nu$ can be calculated using equations (Kjeldsen & Bedding 1995)

* E-mail: yangwuming@hpu.edu.cn

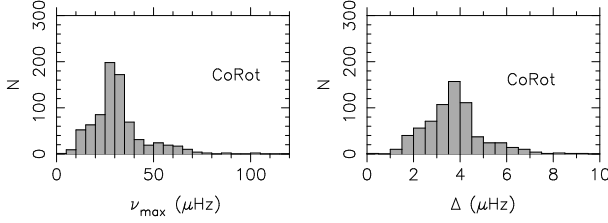


Figure 1. The histogram of the ν_{max} and $\Delta\nu$ obtained by Hekker et al. (2009).

$$\nu_{max} = 3050 \frac{M/M_{\odot}}{(R/R_{\odot})^2 \sqrt{T_{eff}/5777K}} \mu\text{Hz}, \quad (1)$$

and

$$\Delta\nu = 134.9 \frac{(M/M_{\odot})^{1/2}}{(R/R_{\odot})^{3/2}} \mu\text{Hz}. \quad (2)$$

Thus we can obtain the theoretical distributions of ν_{max} and $\Delta\nu$ by simulating the distributions of stellar mass, radius and effective temperature.

Using the stellar population synthesis code TRILEGAL, Miglio et al. (2009) identified that the oscillating giants observed by CoRoT are primarily red-clump stars, i.e. post-flash core-He-burning (CHeB) stars and found that theoretical distributions of ν_{max} and $\Delta\nu$ are in good global agreement with observed ones. Equations 1 and 2 show that the theoretical distributions of ν_{max} and $\Delta\nu$ are relative to the mass and radius distributions of population. Thus Miglio et al. (2009) suggested that mass-loss rate during the red-giant branch (RGB) and star formation rate may affect the distributions of the ν_{max} and $\Delta\nu$.

In this paper, we focused the effects of mass loss, binary interactions, the mixing-length parameter, etc. on the distributions of ν_{max} and $\Delta\nu$. We used the Hurley rapid single and binary evolution codes (Hurley, Pols, & Tout 2000; Hurley, Tout & Pols 2002) to construct stellar models. In Hurley's codes, mass-loss efficiency is an adjustable parameter. Thus they can be applied to studying the effect of mass loss on the distributions of ν_{max} and $\Delta\nu$ of CHeB stars.

The paper is organized as follows. We simply show our stellar population synthesis method in section 2. The results are represented in section 3. In section 4, we discuss and summarize the results.

2 STELLAR POPULATION SYNTHESIS

To simulate the stellar population observed ν_{max} and $\Delta\nu$ (Hekker et al. 2009), we calculated single-star stellar population (SSP) and binary-star stellar population (BSP), respectively. Stellar samples are generated by the Monte Carlo simulation. The basic assumptions for the simulations are as follows. (i) Star formation rate (SFR) is assumed to be a constant over the past 15 Gyr. (ii) The age-metallicity relation is taken from Rocha-Pinto et al. (2000a). (iii) The lognormal initial mass function (IMF) of Chabrier (2001) is adopted. Additionally, for BSP, we generate the mass of the primary, M_1 , according to the IMF. The ratio (q) of the mass of the secondary to that of the primary is assumed to be an uniform distribution within 0-1 for simplicity. Then the mass of the secondary star is given by qM_1 . We assume that all stars are members of binary systems and that the distribution of separations is constant in log a for wide binaries and falls off smoothly at close separation:

$$an(a) = \begin{cases} \alpha_{sep}(a/a_0)^m & a \leq a_0; \\ \alpha_{sep}, & a_0 < a < a_1, \end{cases} \quad (3)$$

where $\alpha_{sep} \approx 0.070$, $a_0 = 10R_{\odot}$, $a_1 = 5.75 \times 10^6 R_{\odot} = 0.13\text{pc}$ and $m \approx 1.2$. This distribution implies that the numbers of wide binary system per logarithmic interval are equal, and that approximately 50% of the stellar systems are binary systems with orbital periods less than 100 yr (Han, Podsiadlowski, & Eggleton 1995). With assumptions mentioned above, we calculated the evolutions of 10^6 stars with an initial mass between 0.8 and $5.8 M_{\odot}$ and mixing-length parameter $\alpha = 2.0$. The theoretical ν_{max} and $\Delta\nu$ of single and binary stars are calculated using equations (1) and (2).

3 CALCULATION RESULTS

3.1 Mass-loss effect

Fig. 2 shows the distributions of mass and radius of CHeB stars of the simulated SSP with different Reimers (Reimers 1975) mass-loss efficiency (η). The distributions of initial mass of progenitors of the CHeB stars also are shown in Fig. 2. Reimers mass loss mainly affects the stars with initial mass less than $2 M_{\odot}$. With the increase in the η , the mass lost by a star during the RGB increases, which leads to many low-mass stars can not evolve into the CHeB stage; and the lower limit of initial mass of the stars being able to evolve into the CHeB stage increases too. For example, when the value of η increases from 1.0 to 2.0, the lower limit increases from about $0.95 M_{\odot}$ to $1.25 M_{\odot}$. Thus the fraction of low-mass CHeB stars and the sample size of the simulated CHeB stars decreases with increasing η . For $\eta = 2.0$, the mass distribution is almost uniform. Moreover, the distribution of logarithmic radius has a fixed peak location between 1.05 and 1.15, which is almost not affected by the mass loss.

The distributions of ν_{max} and $\Delta\nu$ of the simulated CHeB stars with various η are represented in Fig. 3. Both distributions have a dominant peak. But the peak locations are slightly lower than those of the observed distributions. With the increase in η , the number of the CHeB stars with ν_{max} between about $10\sim 30 \mu\text{Hz}$ and $\Delta\nu$ between about $1\sim 4 \mu\text{Hz}$ decreases. However, the dominant peak for $\Delta\nu$ locates between $3\sim 3.5 \mu\text{Hz}$; the effect of the mass loss on the $\Delta\nu$ is not enough to change the peak location. For $\eta \leq 1$, the dominant peak of ν_{max} locates between $25\sim 30 \mu\text{Hz}$. However, when the η increases from 1.0 to 2.0, the peak location of ν_{max} moves to between $20\sim 25 \mu\text{Hz}$.

The changes in the distributions of ν_{max} and $\Delta\nu$ in Fig. 3 should not be due to the typical variations in Monte Carlo simulations. In order to show the effect of sample size on the distributions of ν_{max} and $\Delta\nu$, we calculated the evolutions of 10^6 stars which produced 3973 CHeB stars and the evolutions of 2×10^5 stars which given 793 CHeB stars. Both samples have the same evolutionary parameters. Figure 4 shows that the distributions of ν_{max} and $\Delta\nu$ of the two samples are very similar. A Kolmogorov-Smirnov test shows that the discrepancies between the two sample distributions are not significant: the Kolmogorov-Smirnov statistic $D \simeq 0.030$ for ν_{max} and 0.033 for $\Delta\nu$, and the significance level of the D is 0.61 for ν_{max} and 0.45 for $\Delta\nu$.

In Fig. 5, we plotted the distributions of ν_{max} and $\Delta\nu$ of the simulated CHeB stars with different η as a function of stellar age. For age > 2 Gyr, Fig. 5 shows that the value of ν_{max} and $\Delta\nu$ of CHeB stars is mainly located in the range of $\sim 10 - \sim 30 \mu\text{Hz}$ and $\sim 1 - \sim 4 \mu\text{Hz}$, respectively; moreover, most stars are located around the upper boundary of the distributions. These stars are close to

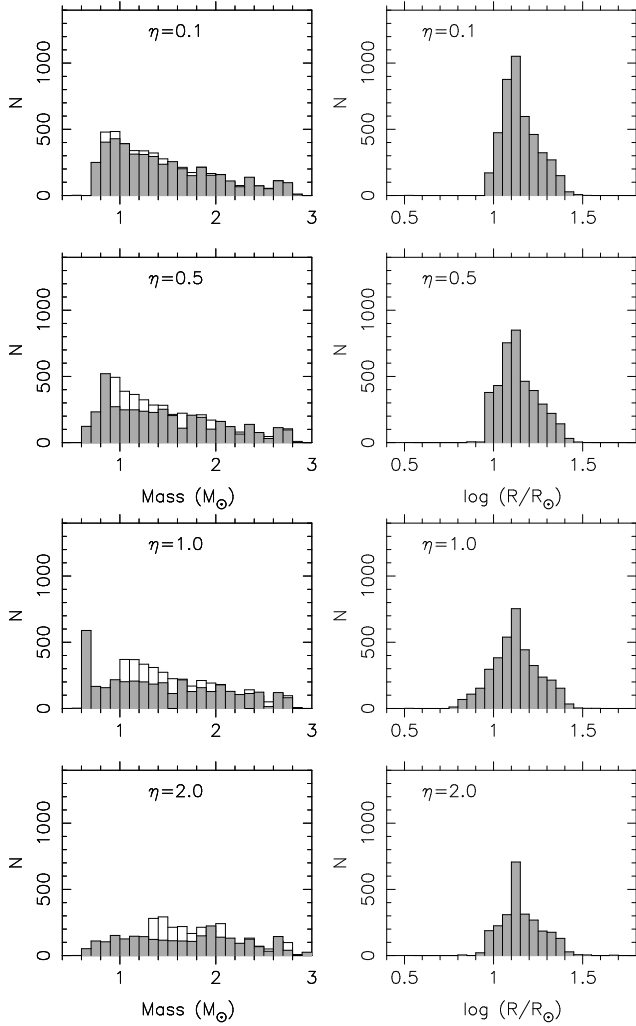


Figure 2. The histograms of mass and radius of CHeB stars of simulated SSP with different mass-loss coefficient η . In the left panels, empty bars illustrate the mass distribution of the progenitors of the CHeB stars.

the zero-age horizontal branch (ZAHB) in the Hertzsprung-Russell (HR) diagram. While the stars around the lower boundary are approaching the asymptotic giant branch (AGB). The CHeB stars with higher ν_{max} and $\Delta\nu$ are mainly from the young population with age less than 2 Gyr. Additionally, Fig. 5 clearly indicates that Reimers mass loss mainly affects the ν_{max} and $\Delta\nu$ of old stars. A big mass-loss rate impedes the low-mass low-metal stars evolving into CHeB stage. Thus for $\eta = 0.5, 1.0$ and 2.0 , the fraction of the CHeB stars with age larger than 12, 10 and 5 Gyr is negligible, respectively. However, the mass loss has almost no effect on the distributions of ν_{max} and $\Delta\nu$ of the stars with age < 2 Gyr. When η increases from 0.5 to 1.0, the upper boundary of ν_{max} and $\Delta\nu$ of the CHeB stars with age between about 7-10 Gyr is enhanced, but the effect of the increase in the η on the distributions of ν_{max} and $\Delta\nu$ of the stars with age between around 2-7 Gyr are not significant. When η increases to 2.0, the upper boundary of ν_{max} and $\Delta\nu$ of the stars with age approximately 5 Gyr increase too, but the distributions of ν_{max} and $\Delta\nu$ of the stars with age between about 2-4.5 Gyr move down slightly, which leads to the peak location of histogram of ν_{max} moves to 20-25 μHz .

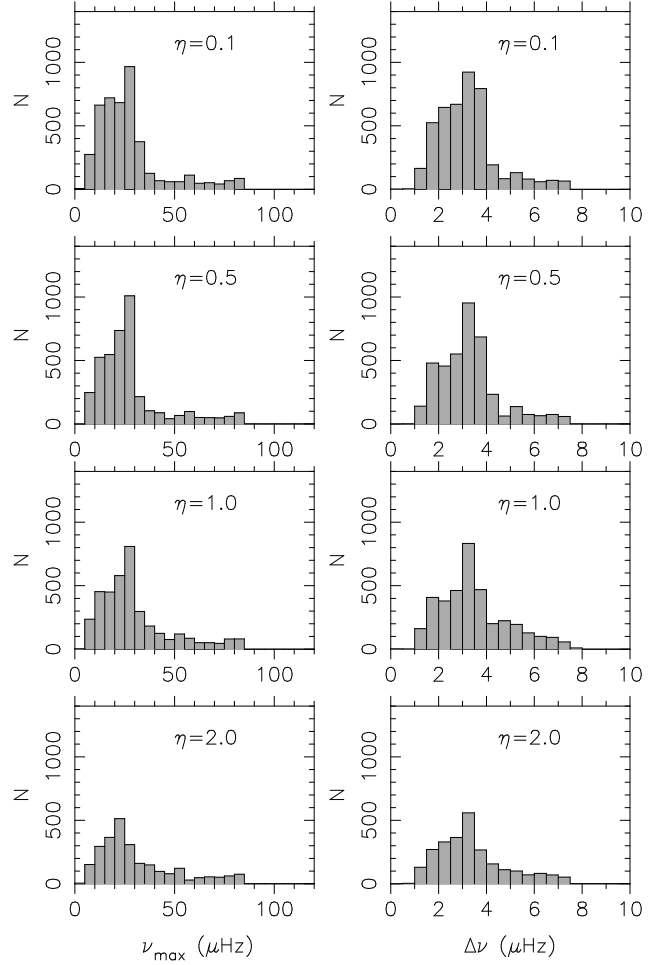


Figure 3. The histograms of ν_{max} and $\Delta\nu$ of CHeB stars of simulated SSP with different mass-loss coefficient η .

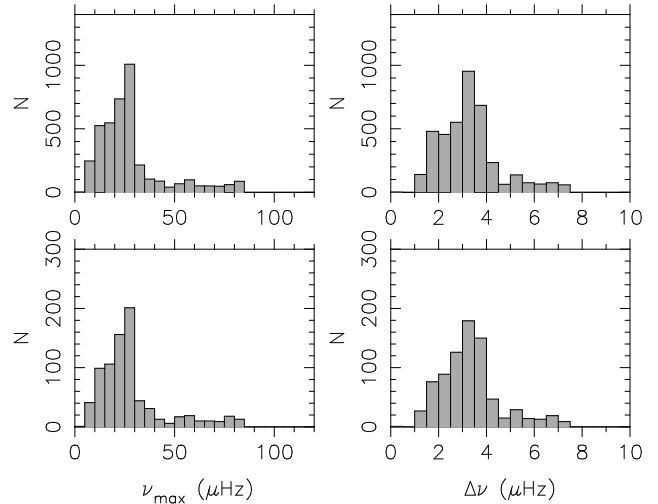


Figure 4. Histogram showing the effect of sample size on the distributions of ν_{max} and $\Delta\nu$ of simulated CHeB stars. Upper panels show the results of 10^6 model evolutions. While lower panels represent the results of 2×10^5 model evolutions. Both samples have the same other parameters. A K-S test shows that the discrepancies between two distributions are insignificant.

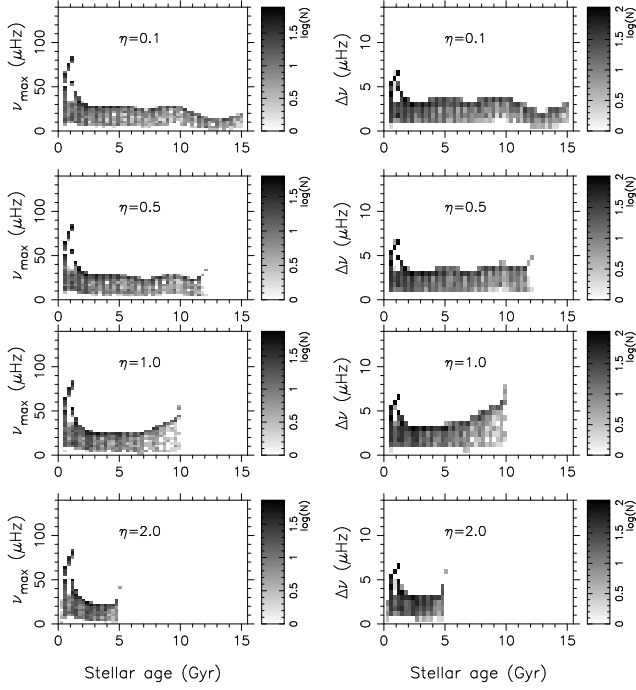


Figure 5. The distributions of the ν_{max} and $\Delta\nu$ of simulated CHEB stars with different η as a function of age.

3.2 BSP effect

Fig. 6 shows the histograms of ν_{max} and $\Delta\nu$ of CHEB stars of the simulated BSP with $\eta = 0.5$ and the distributions of the ν_{max} and $\Delta\nu$ as a function of stellar age. The distributions of ν_{max} and $\Delta\nu$ of CHEB stars of the BSP are very similar to those of the SSP with the same η . This is because that most binary stars evolved into CHEB stage are wide binary stars. Binary interactions such as mass transfer and mass accretion do not take effect in these wide binary stars. However, the lower panels of Fig. 6 show that the value of ν_{max} and $\Delta\nu$ of some stars with age > 2 Gyr is larger than $40 \mu\text{Hz}$ and $4 \mu\text{Hz}$, respectively. This is due to the fact that binary interactions lead to an obvious increase or decrease in the mass of the stars when they evolve into the CHEB stage. Consequently, the ν_{max} and $\Delta\nu$ of these stars are larger than those of the wide binary stars. However, the fraction of these stars is very small. Thus the effect of binary interactions on the distributions of ν_{max} and $\Delta\nu$ is not significant.

3.3 SFR effect

The star formation rate of the Galaxy is not a constant. Rocha-Pinto et al. (2000b) gave that the SFR of the Galaxy at 2–5 Gyr ago is about 2 times larger than an average SFR over the past 15 Gyr and the SFR of the Galaxy at 7–9 Gyr ago is around 1.5 times larger than the average SFR. Fig. 7 shows the distributions of ν_{max} and $\Delta\nu$ of CHEB stars of the simulated SSP with a constant SFR and with the Galaxy SFR given by Rocha-Pinto et al. (2000b). Although the number of simulated CHEB stars is changed, the distributions are similar. In fact, for $\eta = 0.5$, Fig. 5 shows that the value of ν_{max} and $\Delta\nu$ of the CHEB stars with age > 2 Gyr is mainly located in the range of 10–30 μHz and 1–4 μHz , and gathers around 25 μHz and 3 μHz , respectively. Thus increasing or decreasing the SFR of stars at a certain age > 2 Gyr can increase or decrease the

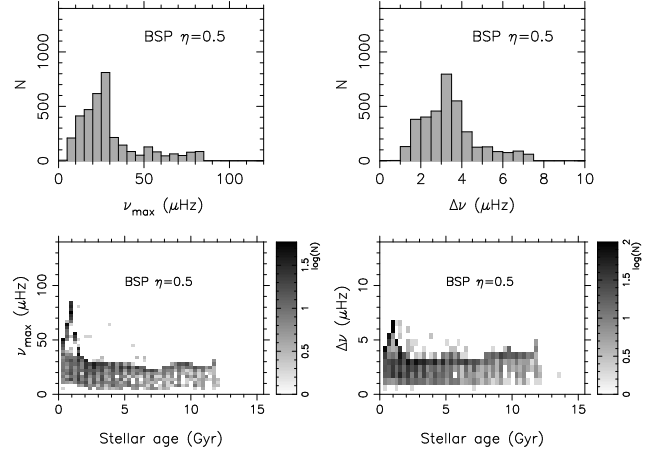


Figure 6. Upper panels show the histograms of ν_{max} and $\Delta\nu$ of CHEB stars of simulated BSP. Here, $\eta = 0.5$. Lower panels indicate the distributions of the ν_{max} and $\Delta\nu$ as a function of stellar age.

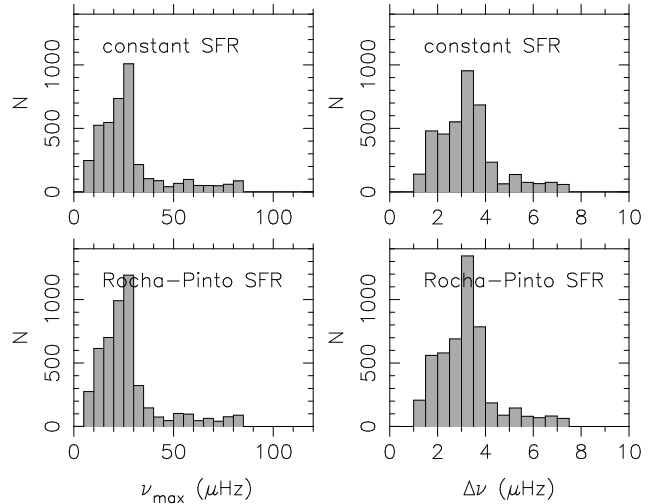


Figure 7. The histograms of ν_{max} and $\Delta\nu$ of simulated CHEB stars for different star formation rate. Here, $\eta = 0.5$. Upper panels show the results of SSP with constant SFR. While lower panels represent the results of SSP with the Galaxy SFR given by Rocha-Pinto et al. (2000b).

number of CHEB stars but not affect the peak location of ν_{max} and $\Delta\nu$ of the CHEB stars. Increasing the SFR of the young stars with age between 0–2 Gyr can increase the number of stars with relatively high ν_{max} and $\Delta\nu$, but also not affect the peak location unless the SFR is enhanced many times.

3.4 Mixing-length parameter effect

The distributions of radius and $\Delta\nu$ of simulated CHEB stars have a dominant peak but the distribution of mass of the simulated CHEB stars with $\eta = 2.0$ has not a dominant peak, which implies that the nonuniform distributions of ν_{max} and $\Delta\nu$ may be caused by the radius of many CHEB stars concentrating in a narrow interval. In fact, equations 1 and 2 indicate that the ν_{max} and $\Delta\nu$ are more sensitive to the change in radius than that in mass. Furthermore, a variation of the mixing-length parameter α mainly changes the stellar radius, but has almost no influence on the luminosity (Kippenhahn & Weigert 1990). Used the Eggleton’s stellar evolu-

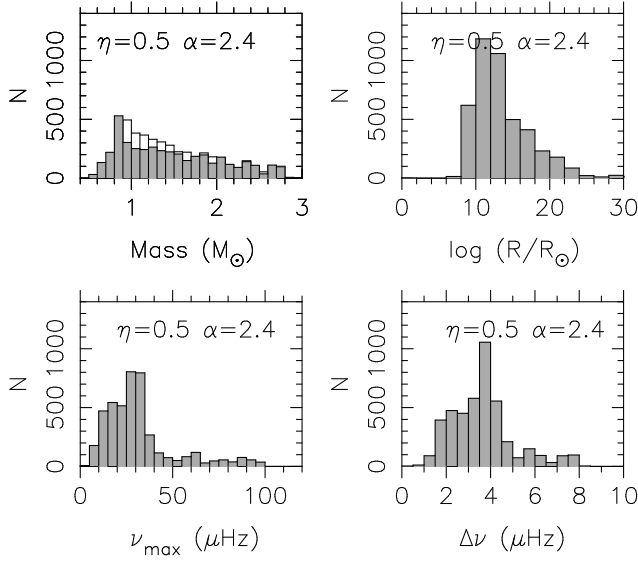


Figure 8. The histograms of ν_{max} , $\Delta\nu$, M , and R of CHeB stars of the simulated SSP with the mixing-length parameter $\alpha = 2.4$.

tion code (Eggleton 1971, 1972, 1973), our calculations show that the increase in α leads to a decrease in the radius of stars evolved into horizontal branch, and thus leads to an increase in ν_{max} and $\Delta\nu$ of the stars. In order to study the effect of the mixing-length parameter α on the distributions of ν_{max} and $\Delta\nu$, we modified the Hurley’s single evolution code to calculate the stellar evolution with $\alpha = 2.4$. Fig. 8 shows the histograms of mass, radius, ν_{max} and $\Delta\nu$ of the simulated CHeB stars with $\alpha = 2.4$. A increase in α results in a movement of the peak location of the radius distribution towards a lower value, and thus leads to a movement towards a higher value for the peak locations of the ν_{max} and $\Delta\nu$ distributions. Furthermore, Fig. 9 represents the distributions of the ν_{max} and $\Delta\nu$ as a function of stellar age. Increasing the mixing-length parameter α leads to the upper boundary of the distributions moving up slightly.

4 DISCUSSIONS AND CONCLUSIONS

Several points should be kept in mind when comparing the theoretical distributions of ν_{max} and $\Delta\nu$ with the observations. Firstly, the scaling equation (1) is obtained from the ideas that ν_{max} is proportional to the acoustic cutoff frequency ν_{ac} and $\nu_{ac} \propto gT_{eff}^{-1/2}$ (Brown et al. 1991), where g is the stellar surface gravity and T_{eff} is the effective temperature. The ν_{max} given by equation (1) is not necessarily accurate (Gilliland 2008; Stello et al. 2009a). For example, the ratio of ν_{ac} of stellar models to that calculated from the global parameters of models is always below unity (see the Figure 8 of Stello et al. (2009a)). However, the scaling equation (2) is very accurate. The uncertainty of equation (2) is within a few per cent (Stello et al. 2009a,b). In addition, scaling equations (1) and (2) agree within a few per cent with stellar model calculations for cool models ($T_{eff} \lesssim 6400$ K) (Stello et al. 2009a). A few per cent deviations in equations (1) and (2) can not obviously change the peak locations of ν_{max} and $\Delta\nu$ in our simulations. Thus the deviations can not affect our basic results.

The giant stars observed by the CoRoT may contain the first giant branch stars. Our simulations show that the distributions of ν_{max} and $\Delta\nu$ of the first giant branch are uniform. Thus the ν_{max} and $\Delta\nu$ of the first giant branch do not affect the peak locations.

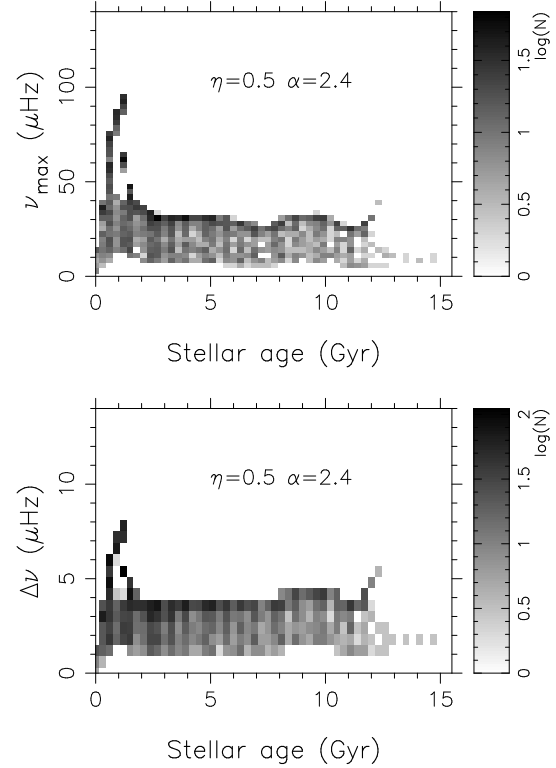


Figure 9. The distributions of ν_{max} and $\Delta\nu$ of CHeB stars of the simulated SSP with $\alpha = 2.4$ as a function of stellar age.

Comparing with the Miglio et al. (2009)’s simulation, we used the same IMF and age-metallicity relation. In our simulation, the SFR is a constant over the past 15 Gyr. But it is a constant over the past 9 Gyr in the Miglio et al. (2009)’s simulation. This difference could not affect the simulated results because the oldest population are impeded into the CHeB stage by mass loss. For example, for $\eta = 1.0$, the simulated population do not contain the stars older than about 10 Gyr. The frequencies of our simulated peak locations are lower than those of Miglio et al. (2009). This may be caused by mixing-length parameter.

For different η , the CHeB stars with age < 2 Gyr lose only a negligible amount of mass from their surface before they evolved into CHeB stage. Thus the effect of the mass loss on the evolution of these stars is insignificant. The distributions of ν_{max} and $\Delta\nu$ of these stars are almost not affected by Reimers mass loss. But for old population, the bigger the η , the more the mass loss. For a big η , the stars lose an appreciable, but from star to star different, amount of mass from their surface before the helium flash. Then the stars move to the left of the HR diagram with slightly decreasing luminosity after the flash; and the mean density of the stars is enhanced. The increase in the mean density leads to that the ν_{max} and $\Delta\nu$ of these stars increase. However, the change in the mean density is different from star to star. The mass of the stars evolved into CHeB at the same age is approximate, but the extent of central helium burning is different. The stars around the ZAHB have a smaller radius than the stars approaching the AGB. The fractional change caused by mass loss in the radius of the stars around the ZAHB is larger, and the change in the mean density of these stars is also larger than those of the stars approaching the AGB. Those stars which are close to the ZAHB are located around the upper boundary of the distributions of ν_{max} and $\Delta\nu$ with age, while the

stars approaching the AGB are located around the lower boundary. Thus the changes of the upper and lower boundary shown in Fig. 5 are different. However, for the middle age population, the stars lose only a little amount of mass from their surface before the helium flash, which almost not affect the radius and luminosity of the stars after the flash. Because the mass decrease slightly but the radius is almost not changed, the mass loss results in that the ν_{max} and $\Delta\nu$ of these stars decrease slightly.

The Reimers mass loss mainly affects the old population. The mass loss leads to an increase in the ν_{max} and $\Delta\nu$ of old population. But a high mass-loss rate can impede the low-mass low-metal stars evolving into CHeB stage. If the Reimers mass loss is very efficient during the red-giant branch, the ν_{max} and $\Delta\nu$ of CHeB stars would not be observed in old clusters. The asteroseismical observation on old clusters may provide a help to constrain the mass-loss rate.

For $\eta = 0.5$, the value of ν_{max} and $\Delta\nu$ of population with age > 2 Gyr is almost located in the range of 10-30 μHz and 1-4 μHz , and gathers about 25 μHz and 3 μHz , respectively. Thus increasing or decreasing the number of stars at a certain age > 2 Gyr can not affect the peak locations of the ν_{max} and $\Delta\nu$. So the peak locations are not sensitive to the SFR and whether population contains old stars. For $\eta = 1.0$, increasing the SFR of stars with age between 7-9.5 Gyr can increase the stars with $\nu_{max} > 25 \mu\text{Hz}$ and $\Delta\nu > 3 \mu\text{Hz}$. But even enhancing the SFR to several times, the peak locations are not affected.

In BSP, some CHeB stars can lose a little mass, but some stars can accrete a little mass by the weak binary interactions. The effect of a little bit of mass loss or accretion before the helium flash on the luminosity and radius of CHeB stars after the flash is negligible. Thus the ν_{max} and $\Delta\nu$ of the CHeB stars which lost a little bit of mass decrease; whereas those of the CHeB stars which accreted a little mass increase. Thus the distributions of ν_{max} and $\Delta\nu$ of CHeB stars can not be affected. However, for the strong binary interactions, on the one hand, some stars which have lost an appreciable amount of mass from their surface would move to the left of the H-R diagram with slightly decreasing luminosity, at the same time, the mean density of these stars would increase, thus the ν_{max} and $\Delta\nu$ of these stars increase; on the other hand, some stars with age > 2 Gyr which have accreted a considerable amount of mass would become like the stars with age < 2 Gyr, thus their ν_{max} and $\Delta\nu$ can increase obviously too. However, the fraction of these interactive binary stars appearing in our simulated CHeB stars is very small. Consequently, although the binary interactions such as mass transfer and mass accretion can affect the ν_{max} and $\Delta\nu$ of CHeB stars undergoing a mass accretion or mass loss, the effect of binary interactions on the distributions of the ν_{max} and $\Delta\nu$ of CHeB stars is not significant.

An increase in the mixing-length parameter α mainly leads to a decrease in the radius of all CHeB stars after the helium flash. Thus the ν_{max} and $\Delta\nu$ of CHeB stars increase with α . Consequently, the peak locations of the ν_{max} and $\Delta\nu$ can be affected by the α . For the middle-age population with age between about 2-5 Gyr, the peak locations are more sensitive to the α than mass-loss rate, SFR and metal abundance. Thus the asteroseismical observation on the middle age clusters may provide a help to constrain the mixing-length parameter.

The mass of simulated CHeB stars is mainly located in 1-2 M_{\odot} . For the CHeB stars with the mixing-length parameter $\alpha = 2.0$, the most of these stars have a radius between about 11-14 R_{\odot} . Thus even the mass distribution is uniform, the stars have an approximate mean density. Thus they have an approximate ν_{max} and

$\Delta\nu$. Consequently, there is a dominant peak in the distributions of the ν_{max} and $\Delta\nu$.

A high Reimers mass loss can lead to an increase in the ν_{max} and $\Delta\nu$ of old population, but a very small decrease in that of middle-age population, and impedes the low-mass low-metal stars evolving into CHeB stage. However, the mass loss does almost not affect the ν_{max} and $\Delta\nu$ of young population. The effect of the Reimers mass loss on the peak locations of ν_{max} and $\Delta\nu$ of the CHeB stars is not significant unless the mass-loss rate is very high. The effect of star formation rate and binary interactions on the peak locations of ν_{max} and $\Delta\nu$ of the CHeB stars is also not significant. The dominant peak of ν_{max} and $\Delta\nu$ is due to the fact that most of CHeB stars have an approximate radius. The radius can be affected by the mixing-length parameter. Thus the peak location also can be affected by the mixing-length parameter.

ACKNOWLEDGMENTS

We thank the anonymous referee for his/her helpful comments. This work was supported by the Ministry of Science and Technology of the Peoples republic of China through grant 2007CB815406, by the NSFC through grants 10773003, 10933002, 10963001, and by the high-performance grid computing platform of Henan Polytechnic University.

REFERENCES

- Baglin, A., Michel, E., Auvergne, M., The COROT Team., 2006, in Proceedings of SOHO 18/GONG 2006/HELAS I, Beyond the spherical Sun (ESA SP-624). 7-11 August 2006, Sheffield, UK. Editor: K. Fletcher, P34
- Barban, C., De Ridder, J., & Mazumdar, A. et al., 2004, in Proceedings of the SOHO 14 / GONG 2004 Workshop (ESA SP-559). "Helio- and Asteroseismology: Towards a Golden Future". 12-16 July, 2004. New Haven, Connecticut, USA. Editor: D. Danesy, p.113
- Bedding, T. R., Kjeldsen, H., Butler, P. R. et al., 2004, ApJ, 614, 380
- Bedding, T. R., Huber, D., Stello, D., 2010, ApJ, 713, L176
- Brown, T. M., Gilliland, R. L., Noyes, R. W., Ramsey, L. W., 1991, ApJ, 368, 599
- Chabrier, G. 2001, ApJ, 554, 1274
- Carrier, F., Eggenberger, P., Bouchy, F., 2005, A&A, 434, 1085
- De Ridder, J., Barban, C., Carrier, F. et al. 2006, A&A, 448, 689
- Edmonds, P. D., Gilliland, R., 1996, ApJ, 464, L157
- Eggenberger, P., Carrier, F., Bouchy, F. Blecha, A. 2004, A&A, 422, 247
- Eggenberger, P., Carrier, F., Bouchy, F., 2005, NewA, 10, 195
- Eggenberger, P., Carrier, F., 2006, A&A, 449, 293
- Eggleton, P. P., 1971, MNRAS, 151, 351
- Eggleton, P. P., 1972, MNRAS, 156, 361
- Eggleton, P. P., 1973, MNRAS, 163, 279
- Frandsen, S., Carrier, F., Aerts, C. et al., 2002, A&A, 394, L5
- Frandsen, S., Bruntt, H., Grundahl, F., 2007, A&A, 475, 991
- Gilliland, R. L., Brown, T. M., & Kjeldsen, H. et al., 1993, ApJ, 106, 2441
- Gilliland, R. L., 2008, ApJ, 136, 566
- Han Z., Podsiadlowski P., Eggleton P.P., 1995, MNRAS, 272, 800
- Hekker, S., Kallinger, T., Baudin, F. et al., 2009, A&A, 506, 465
- Hurley, J. R., Pols, O. R., Tout, C. A., 2000, MNRAS, 315, 543

- Hurley, J. R., Tout, C. A., Pols, O. R., 2002, MNRAS, 329, 897
- Kippenhahn, R., Weigert, A., 1990, in *Stellar Structure and Evolution* (Berlin, Springer-Verlag), p271
- Kjeldsen, H., Bedding, T. R., 1995, A&A, 293, 87
- Kjeldsen, H., Bedding, T. R., Butler, R. P. et al., 2005, ApJ, 635, 1281
- Miglio, A., Montalbán, J., Baudin, F. et al., 2009, A&A, 503, L21
- Reimers, D. 1975, *Memoires of the Societe Royale des Sciences de Liege*, 8, 369
- Rocha-Pinto, H. J., Maciel, W. J., Scalo, J., Flynn, C., 2000a, 358, 850
- Rocha-Pinto, H. J., Scalo, J., Maciel, W. J., Flynn, C., 2000b, 358, 869
- Stello, D., Bruntt, H., Kjeldsen, H. et al., 2007, MNRAS, 377, 584
- Stello, D., Gilliland, R. L., 2009, ApJ, 200, 949
- Stello, D., Chaplin, W. J., Basu, S., Elsworth, Y., Bedding, T. R., 2009a, MNRAS, 400, L80
- Stello, D. et al., 2009b, ApJ, 700, 1589
- Stello, D., Basu, S., Bruntt, H., 2010, ApJ, 713, L182
- Yang, W., Meng, X., 2010, NewA., 15, 367